JOURNAL OF RESEARCH of the National Bureau of Standards—A. Physics and Chemistry
Vol. 71A, No. 5, September–October 1967

Surface-Layer Relaxation in the Dielectric Spectrum of CaF_2 Doped With GdF_3

A. D. Franklin, S. Marzullo, and J. B. Wachtman, Jr.

Institute for Materials Research, National Bureau of Standards, Washington, D.C. 20234

(May 10, 1967)

CaF_2 crystals doped with 0.1 percent GdF_3 were observed to develop surface layers when annealed above 700 °C in air, during application of Pt paste electrodes. The conductivity in these surface layers was much higher than in the bulk, due presumably to the large numbers of anion vacancies produced by dissolved oxygen. The presence of these high conductivity surface layers produced a relaxation in the dielectric spectrum with (1) an approximately temperature-independent magnitude, $\Delta\kappa$, (2) a relaxation time controlled by the conductivity of the surface layers, and influenced therefore by heat treatment of the specimen, and (3) an activation energy equal to that for conductivity of the surface layers, about 0.9 eV. This relaxation is sufficiently similar to dielectric relaxations observed previously in ionic crystals and ascribed to defect pairs to suggest that great care must be taken in interpreting dielectric measurements in these materials. What is thought to be dipole relaxation may in fact be due to the presence of thin layers accidentally present on the crystal. There is a marked electrode polarization effect in these crystals. The electrode capacitance at not-too-low frequencies depended upon the frequency and both the number and mobility of the charge carriers with 3/2 power laws.

Key Words: CaF_2, conductivity, crystals, defect pairs, dielectric relaxation, electrode capacitance, surface layers.

1. Introduction

Dielectric relaxation has been an important tool in studying point defect pairs in ionic crystals. Considerable work has been done on divalent cations (anions) paired with cation (anion) vacancies in alkali halides [1].[1] More recently, such dipole relaxation ascribed to impurity cations paired with interstitial fluoride ions has been reported [2] in CaF_2 doped with trivalent cations. This interpretation of the dielectric relaxation data as due to coupled pairs of defects rests on several grounds: most notably, comparison between doped and pure crystals; the observation of a single relaxation time, to be expected from reorienting independent dipoles; the observation of activation energies that are (1) similar to but somewhat lower than the activation energies for d-c conduction in the same compounds, and (2) of the same general magnitude as activation energies calculated for coupled defect reorientation on theoretical grounds; and, in several cases, examination of the same crystal by dielectric relaxation and spin resonance or by dielectric and an elastic relaxation.

The unambiguous interpretation of the dielectric relaxation can be somewhat complicated by the existence of several other effects, arising from other causes but giving rise to very similar data. In particular, when two distinct phases are present, with different conductivities and dielectric constants, a dielectric relaxation can be observed. If the minor phase is distributed as dispersed particles of uniform shape [3], or if it forms a thin layer [4], the resulting relaxation will obey the Debye equations. An examination of possible effects of this sort in materials of interest for coupled-defect studies can therefore help in sorting out the latter effects.

In this spirit, we present here a study of such a relaxation, observed in single-crystal CaF_2 containing 0.1 mole percent GdF_3. Similar layers were formed on pure CaF_2 but were not studied in detail. Thin surface layers of high conductivity were formed by annealing the crystals in air during the application of platinum paste electrodes. Disregarding electrode blocking effects, the specimen could then be represented by the sketch and equivalent circuit in figure 1., B denotes the bulk, l the layer on the surface under the electrodes, and l' the exterior surface layer from electrode to electrode. The parallel impedance of such a circuit exhibits a relaxation describable by the Debye [5] equation with a single relaxation time.

[1] Figures in brackets indicate the literature references at the end of this paper.

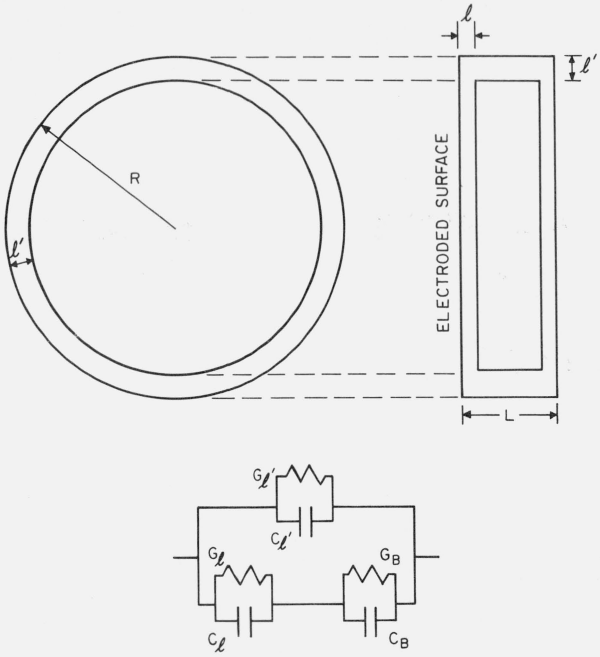

FIGURE 1. *Sketch of layered specimen, with equivalent electrical circuit.*

2. Specimens

Four pieces were cut from a crystal, obtained from the Harshaw Chemical Company, with nominal 0.1 mole percent GdF_3 present. On one, here designated A, gold electrodes were evaporated, and the specimen was subject to no heat treatment. On three, platinum paste was applied in several doses to the major faces, during which the specimens were annealed in air at about 700 °C for each dose. It has been shown [6] that under this sort of anneal oxygen diffuses into CaF_2 and then precipitates as the crystal cools, producing well-defined surface layers containing CaO particles. Similar layers were observed under the microscope in our specimens as shown by figure 2. Table 1 gives dimensions of the specimens, together with the thickness of the surface layers taken as the precipitated zones observed under the microscope. Note that specimen A is essentially free of precipitate while specimen D contains precipitate throughout. The properties of specimen D are therefore some measure of the properties of the surface layers on specimens B and C, while for the properties of their interior portions, between the surface layers, specimen A provides a measure.

3. Comparison Between Observed Behavior and Predictions of the Surface-Layer Model

3.1. Low-Frequency Conductivity

At frequencies well below the critical frequency of the relaxation, but high enough to avoid blocking effects at the electrodes, the apparent conductivity should approach a low-frequency limit given by

$$\sigma = \left\{ \frac{(1-A)\sigma_B + A\sigma_l}{(1-2l/L)\sigma_l + (2l/L)\sigma_B} \right\} \sigma_l \qquad (1)$$

where l is the thickness of the layer under the electrodes, L the total thickness of the specimen, σ_l and σ_B the true conductivities of the surface layer and the bulk, respectively, and

$$A = (l'/R)(2 - l'/R)(1 - 2l/L)$$

with l' the thickness of the layer on the outer edge of the specimen. For l and l' equal to zero (specimen A), σ becomes σ_B, while for $2l$ equal to L (specimen D) σ becomes σ_l.

Specimens B, C, and D were originally very slowly cooled after the anneal involved in applying the Pt electrodes. Figure 3 shows ln (σT) plotted as a function of T^{-1}. Straight lines were drawn through the data for specimens A and D, to produce values for σ_B and σ_l as a function of temperature. These, with the data in table 1, were then inserted into eq (1) to produce estimates of σ for the layered specimens B and C. The lines on figure 3 labeled B and C are the results of these calculations. Although the scatter, much of it in the measuring temperatures, is large, the calculations describe the data reasonably well.

The conductivity of the partially oxidized specimens was found to depend upon the rate of cooling from a temperature above about 500 °C. The effect was studied using specimen C. By removing the specimen from the furnace to provide a rapid cool, the apparent conductivity was increased by almost an order of magnitude, with no apparent change in activation energy. A second slow-cooling returned the apparent conductivity to close to its former value, so that the effect of this heat-treatment is approximately reversible. A similar anneal (at 400 °C) and rapid cooling produced no effect in the gold-electroded specimen.

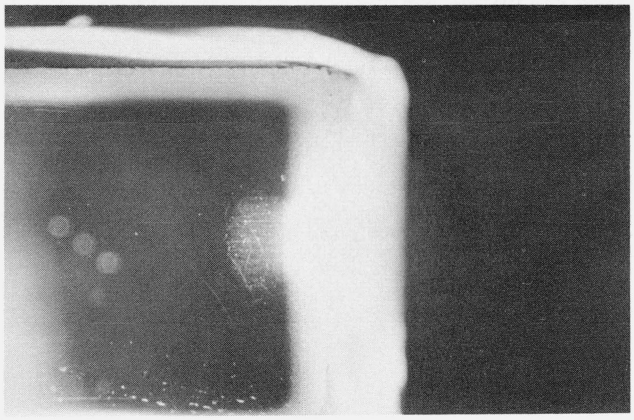

FIGURE 2. *Optical micrograph of cross section of specimen C.*

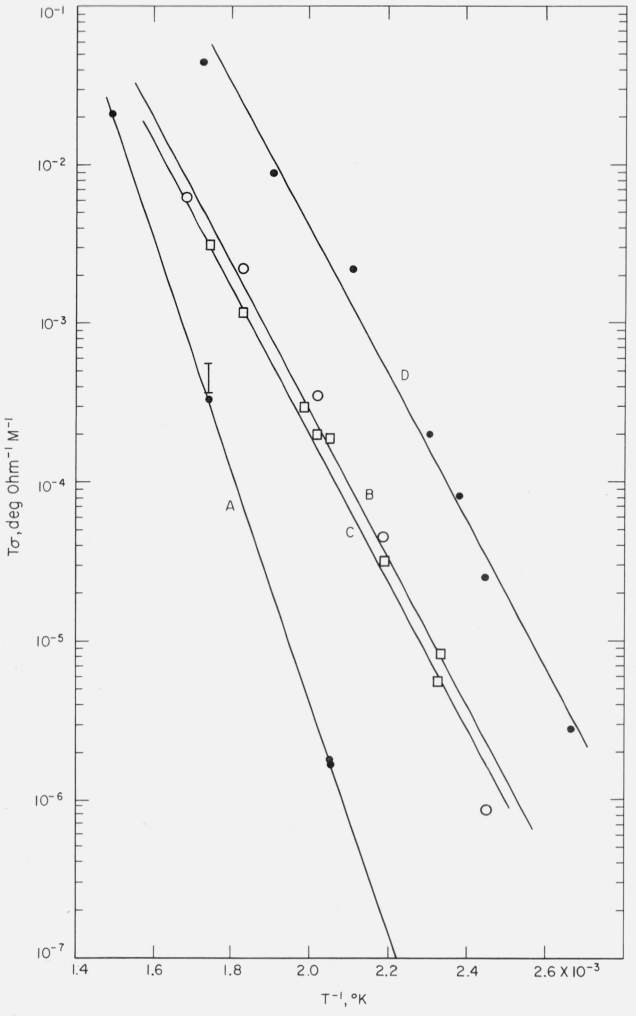

FIGURE 3. *Temperature dependence of apparent low-frequency conductivity of specimens A, B, C, and D.*

3.2. Dielectric Relaxation

The layered model of figure 1 should exhibit a relaxation in the dielectric spectrum with a single relaxation time. In interpreting our data, we assume that the true dielectric constant of the material, κ_T, is the same for all parts of the specimen. Then the model predicts the following:

(i) The high-frequency limit, κ_∞, of the apparent real part of the dielectric constant is

$$\kappa_\infty = \kappa_T. \tag{2}$$

(ii) The magnitude, $\Delta\kappa$, in the dispersion in κ' is

$$\Delta\kappa = \kappa_T(1-l'/R)^2\left\{\frac{(1-2l/L)\sigma_l^2+(2l/L)\sigma_B^2}{[(1-2l/L)\sigma_l+(2l/L)\sigma_B]^2}-1\right\}. \tag{3}$$

With the data in table 1 and σ_l and σ_B derived as in the last section, it is evident the terms in σ_B are negligible, and eq (3) reduces to

$$\Delta\kappa = \kappa_T\frac{(1-l'/R)^2(2l/L)}{(1-2l/L)}. \tag{4}$$

(iii) The relaxation time of the model is

$$\tau = \kappa_T[(1-2l/L)\sigma_l+(2l/L)\sigma_B]^{-1}. \tag{5}$$

Combining eq (5) and eq (1), and again dropping the negligibly small terms in σ_B,

$$\tau = \frac{\kappa_T}{1.13\times10^{11}}\frac{A}{\sigma(1-2l/L)^2} \tag{6}$$

with σ in (ohm · m)$^{-1}$ and τ in sec. A has the meaning of the last section.

For temperatures from about 135 °C to about 300 °C, a relaxation appeared in the dielectric spectrum of specimens B and C between 20 and 10^5 Hz. Figure 4 shows a plot of the real and the imaginary parts of the parallel dielectric constant for specimen *C* in the slowly cooled condition at 214 °C. These data when plotted as an Argand diagram, in the manner of Cole and Cole [7], are shown in figure 5. Good semicircles

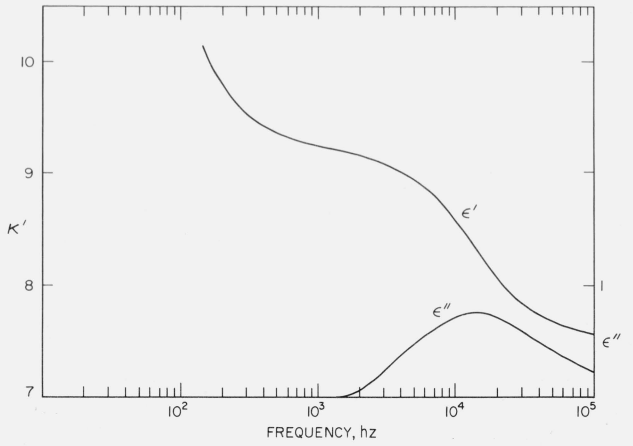

FIGURE 4. *Portion of the dielectric spectrum of specimen C at 214 °C.*

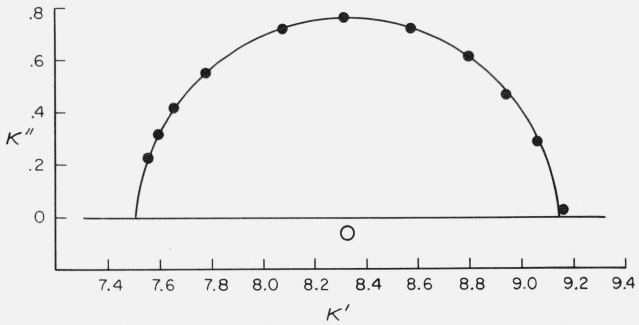

FIGURE 5. *Argand diagram for specimen C at 214 °C.*

were formed in most cases, with approximately single-relaxation-time behavior. Reasonable estimates of κ_∞, the high-frequency dielectric constant, and $\Delta\kappa$, the magnitude of the dispersion, could be obtained from these diagrams. To obtain the relaxation times, τ, of the dispersion, use was made of the Cole-Cole relation in the form

$$\left[\frac{(\kappa_0-\kappa')^2+\kappa''^2}{(\kappa'-\kappa_\infty)^2+\kappa''^2}\right]^{1/2}=(\omega\tau)^{1-\alpha} \tag{7}$$

where κ_0 is the low-frequency limit for the dielectric constant in the Argand diagram and α is a parameter describing the breadth of the distribution of relaxation times. A plot of the left-hand side as a function of the circular frequency, ω, produces a straight line. The value of τ is the inverse of ω when the function on the left equals unity.

Figure 6 shows the temperature dependence of κ_∞, with the data of Rao and Smakula [8] measured at 10^{10} Hz, plotted for comparison. All specimens show roughly the same temperature dependence as do the data of Rao and Smakula, which were measured on pure CaF_2 in the absence of any dispersion effects. The discrepancy between our data and those of Rao and Smakula *could* arise from overestimating the thickness of our specimens, but it seems unlikely that our errors could be as large as required to bring all the data into coincidence. It seems more reasonable to suppose an additional relaxation exists in our dielectric spectra, at frequencies above our measuring range. Defect pairs, such as $Gd^{3+}-F^-$ interstitials, could give rise to such a relaxation.

In figure 7 we show the temperature dependence of $\Delta\kappa$. This dispersion was observed only in specimens B and C, the specimens containing two layers. With specimen A, gold-electroded with no visible oxide layer, a much smaller relaxation with quite different characteristics was observed, but may not be related to that observed in the dielectric spectra of specimens B and C. None was observed with specimen D (fully precipitated).

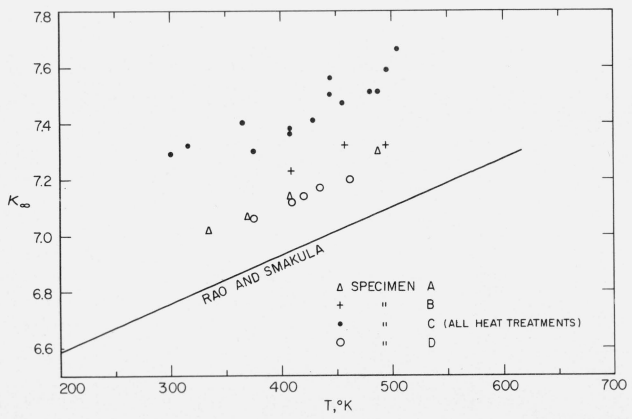

FIGURE 6. *Temperature dependence of κ_∞, the high-frequency limit of the real part of the relative dielectric constant.*

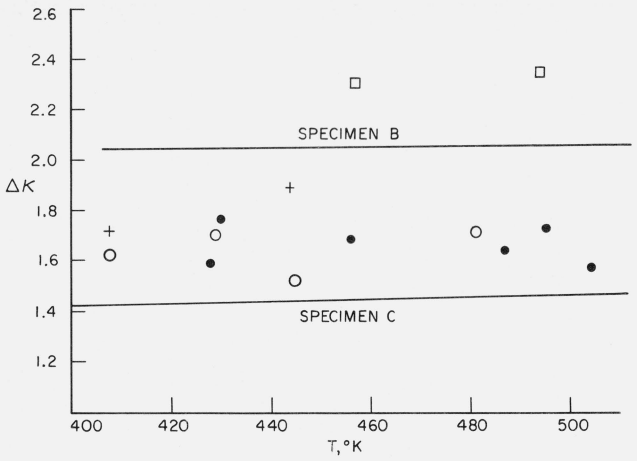

FIGURE 7. *Temperature dependence of $\Delta\kappa$, the magnitude of the dispersion in the real part of the relative dielectric constant, for specimens B and C.*

Specimen B, □; Specimen C, slowly cooled, mild quench ○, rapid quench +.

The lines drawn on figure 7 show values of $\Delta\kappa$ calculated with eq (4) and the appropriate values of κ_∞ substituted for κ_T. The calculations reproduce the general lack of dependence of $\Delta\kappa$ upon temperature, but underestimate the magnitude by 10 to 15 percent. The calculated value for $\Delta\kappa$ depends directly upon the thickness of the layers under the electrodes. The estimate of this thickness by microscopic examinations can easily be in error by this amount, in view of the fact that (1) a judgment must be made as to the edge of the precipitated zone, and (2) the region of high conductivity can be expected to extend inward from the precipitated zone, so that the thickness of the latter must underestimate somewhat the thickness of the *electrical* layer of high conductivity.

A dispersion of this magnitude cannot, on the other hand, be accounted for by $Gd^{3+}-F^-$ interstitial pairs, even if all the Gd ions present were associated with interstitial ions. Use may be made of the simple relation for dipole polarization [9]

$$\Delta\kappa=\frac{n\mu^2}{3kT\epsilon_0} \tag{8}$$

where n is the number of dipoles/cm^3, $\mu=ea$ is the dipole moment, with a the F^-F^- distance, and T is taken as 450 °K; a value of $\Delta\kappa$ of 0.3 results. However, had the surface layers been thinner by a factor of 10, the relaxation arising from their presence would have been of the same order of magnitude as the observed dipole relaxation.

The observed relaxation time of the relaxation found in specimens B and C is closely related to the apparent low-frequency conductivity as called for by eq (6). Figure 8 shows a log-log plot of τ versus $A/(1-2l/L)^2\sigma$ for both specimen B and specimen C heat treated in various ways. Equations 6 and 7 appear in fact to describe these data rather well. The correspondence is in fact very strong. By varying the measurement temperature of specimen C for a given

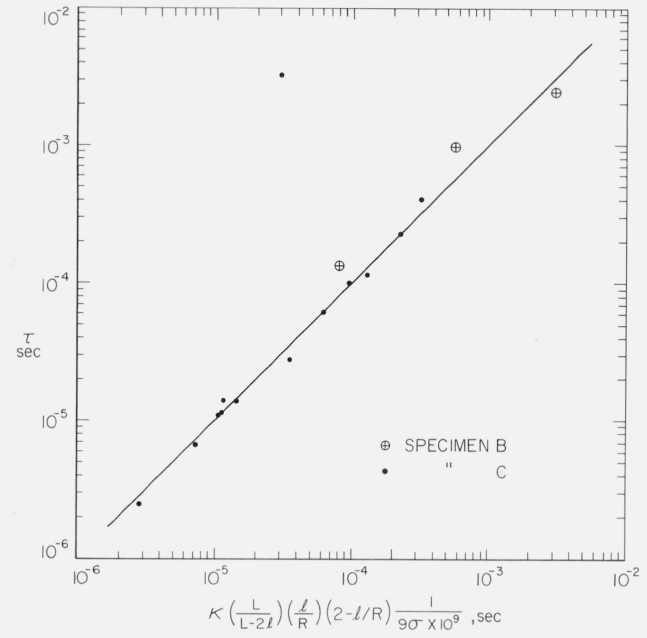

FIGURE 8. *Relation between relaxation time and apparent conductivity in specimens B and C.*

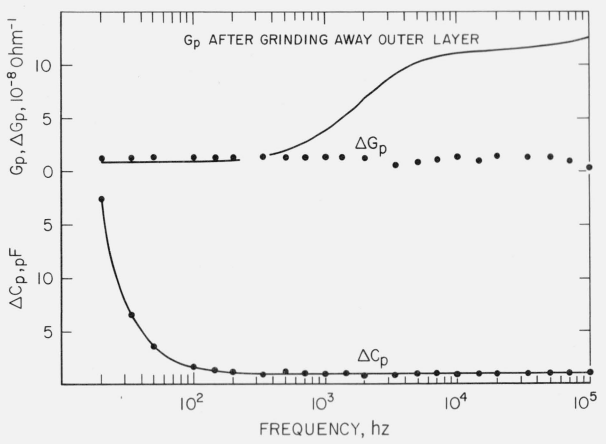

FIGURE 9. *Effect upon parallel capacitance and conductance of grinding away outer surface of layered specimen similar to specimen C.*

Measurements made at 183 °C.

heat-treatment, the mobility of a constant number of charge carriers was varied. Measurements at a given temperature of the specimen with varying heat treatments corresponded to varying the number of charge carriers with constant mobility. Regardless of which mechanism was used to vary σ, eq (6) described the accompanying variation in τ. The result appears completely to rule out dipoles as a source of the relaxation.

According to the model, the cylindrical surface layer on the outside of the specimen contributes the elements represented by $G_{l'}$ and $C_{l'}$ in figure 1. These should have no influence on the relaxation, so that grinding off the layer should reduce both the parallel conductance and the parallel capacitance of the specimens by quantities that are independent of frequency (except at the low frequencies where electrode effects occur). Figure 9 shows the change in parallel capacitance and conductance at 183 °C produced by grinding off this outer surface of a layered specimen, of dimensions similar to specimen C, save for the expected electrode effect in ΔC_p, the changes produced by grinding are frequency independent. The figure also shows the conductance of the specimen after grinding. The relaxation is centered around 115×10^3 Hz. The change in the conductance at low frequencies produced by grinding is larger than the conductance remaining, again in accordance with the model.

The correspondence between the predictions of the layer model and the nature of the dielectric dispersion in these specimens is good. Using layer thickness obtained from microscopic examination and conductivities obtained from specimens composed entirely of one layer or the other, it has been possible to account quantitatively, to within 10 to 15 percent, for the low-frequency conductivity, high-frequency dielectric constant, magnitude of the dispersion, and relaxation frequency.

4. Electrode Polarization

At very low frequencies, as figure 3 demonstrates, a large increase in capacitance occurs with decreasing frequency, accompanied by a decrease in conductance. For not too low frequencies, the capacitance varied as $\omega^{-3/2}$ and the decrease in conductance as $\omega^{-1/2}$, in accordance with Friauf's [10] model for two mobile charge carriers, one of which is blocked at the electrodes, or Ninomiya and Sonoike's [11] model with one blocked carrier. In actual fact, d-c measurements showed that only part of the current is blocked. If only one mobile carrier is present, it is only partially blocked at the electrodes.

Models such as those of Friauf and of Ninomiya and Sonoike suggest that the increment in capacitance depends upon both the density of charge carriers and their mobilities, as well as geometrical factors:

$$\Delta C = \frac{KA}{L^2} f(\mu, n, \omega), \tag{11}$$

where μ is the mobility and n the density of the charge carriers, A the area, L the thickness of the specimen, and K a constant containing the dielectric constant.

The experiments on specimen C, in which quenching could be used to vary the density of the charge carriers independently of their mobility, allow the separate dependence upon n and μ to be studied. Figure 10 shows the log of the slopes of capacitance versus $\omega^{-3/2}$ plots, in the form

$$\frac{L^2}{(\pi R^2)} \frac{\partial C_p}{\partial \omega^{-3/2}}$$

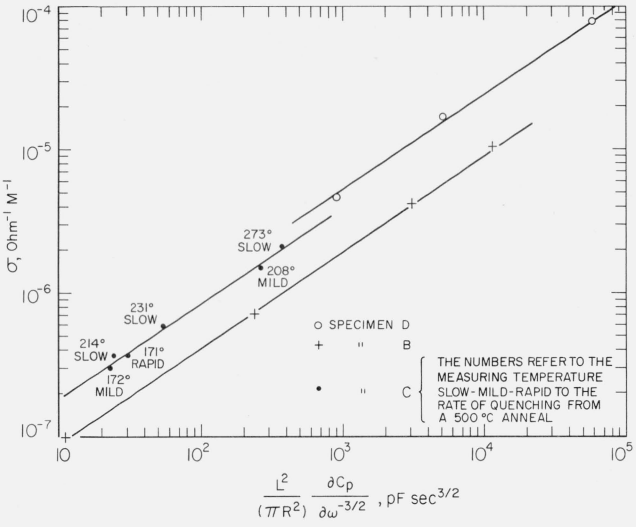

FIGURE 10. *Relation between electrode capacitance and apparent conductivity in specimens B, C, and D.*

plotted versus the log of the apparent conductivity, σ, at frequencies below the relaxation discussed above, but above the onset of the electrode polarization effects discussed here. The data for specimen C show that the electrode polarization effect depends upon σ and not upon n and μ separately. Equation (11) can be written for this specimen

$$\frac{L^2}{A}\,\Delta C = K(n\mu)^{3/2}\omega^{-3/2}. \tag{12}$$

Since in the specimens B and C only the thin outer shell carries appreciable low-frequency current, it seems reasonable to use the area of this shell and the conductivity, σ_l, of the oxidized layers in eq (12) for these specimens. Then using eq (1) to replace σ_l by σ, the apparent conductivity

$$\frac{L^2}{(\pi R^2)}\,\frac{\partial C_p}{\partial \omega^{-3/2}} = \frac{KR\sigma^{3/2}}{(2Rl-l^2)^{1/2}} \tag{13}$$

while for specimen D, with no interior part,

$$\frac{L^2}{(\pi R^2)}\,\frac{\partial C_p}{\partial \omega^{-3/2}} = K\sigma^{3/2}. \tag{14}$$

According to these equations, the lines representing the data for specimens B and C should be separated from that for D by appropriate values of log $R(2Rl-l^2)^{-1/2}$. The following table gives values for $R(2Rl-l^2)^{-1/2}$ calculated from the data in table 1 compared to those derived from the displacements of the lines in figure 9 from the line for specimen D:

Specimen	Calculated	Observed
B	3.8	4.3
C	4.5	1.6

These electrode polarization effects are known to depend rather sensitively upon the nature of the electrode contact. The electrodes were applied to specimens B and D at the same time, both receiving the same series of heat-treatments in the course of applying the electrodes, while specimen C was treated separately. This may account for the reasonable correspondence between calculated and observed factors in the table for specimen B and the discrepancy for specimen C.

The results on specimen C show that ΔC depends upon $\sigma_l^{3/2} = (n\mu)^{3/2}$ and not upon n and μ separately. In a study of alkali halides containing divalent impurities (both anions and cations), Wintle and Rolfe [12] also found a dependence on $\sigma^{3/2}$, but in addition found an independent dependence upon μ, with a negative exponent. This dependence was missing here. It should be noted that our results refer only to the temperature and frequency region in which ΔC exhibited $\omega^{-3/2}$ behavior. At lower frequencies the increase of ΔC with decreasing ω became less rapid. At higher temperatures (above about 250 °C) this effect became more pronounced, and ΔC at temperatures above about 300 °C exhibited an ω^{-1} behavior.

5. Discussion

5.1. Relation to Dipole Relaxation Measurements

The comparison between our experimental data and the behavior expected from the simple surface-layer model establishes clearly the importance of these layers for the electrical properties of these specimens.

In particular, the surface layers are responsible for the presence of a very significant relaxation in the dielectric spectrum. Dielectric relaxation has been extensively used as a means of studying coupled point defects; our results suggest that great care must be taken to eliminate the relaxation due to surface layers from such studies. In the present study, the surface layers were very thick and obvious. Layers with the same properties but thinner by a factor of 10 would be only a few tens of microns thick, and therefore quite easy to overlook, and yet would produce a relaxation comparable to that expected from the approximately 0.1 mole percent of dipoles expected to be present.

The outstanding characteristics of high-conductivity-layer dielectric relaxation are an approximately temerature-independent magnitude, $\Delta\kappa$, and a relaxation time determined by the conductivity of the layer. Since the layer will probably obtain its high conductivity as a result of a high doping level, the activation energy of its conductivity, and hence of the relaxation time, is apt to be the motional activation energy of the majority carrier in the layer. Under special circumstances, which obtained in the present experiments, the layer conductivity may be influenced by thermal treatment of the specimen. This will result in a sensitivity of the relaxation time to thermal treatment.

Published results of dielectric relaxation experiments often exhibit some of these characteristics. The temperature independence of $\Delta\kappa$ is not only com-

mon in these experiments, it is almost the rule. It was remarked upon for NaCl containing $CaCl_2$ by Haven [1b] and for NaCl containing $MnCl_2$ by Watkins [1d]. It is exhibited by the data Dryden and Meakins [1c] for several alkali halides containing divalent cations. The same effect was noted for KBr crystals containing F-centers by Krasnopevtsev [1h], who also observed a decrease in relaxation time with increasing concentration of F-centers, an effect difficult to understand in terms of reorienting dipoles. Jacobs et al. [1f], in a study of KBr containing K_2S, not only found $\Delta\epsilon$ essentially independent of temperature, but also observed that thermal treatment of the samples produced much the same effect as observed here, a shift in the low-frequency conductivity accompanied by an inverse shift in the relaxation time.

Kessler and Mariani [1j] observed in NaCl doped with $CaCl_2$ a high-temperature relaxation, in addition to the one described by Haven and others, the characteristics of which correspond rather well to surface-layer relaxation. The magnitude $\Delta\epsilon$ appeared to be independent of temperature. Increasing the concentration of $CaCl_2$ decreased the relaxation time but did not change $\Delta\epsilon$. It is particularly interesting to note that Kaderka [1i] reports much the same results for NaCl doped with NaOH or $NaCO_3$, except that increasing the concentration of the divalent anion increased the relaxation time. If τ were related to either σ_l or σ_B as in eq (5) and if the dominant conductivity were controlled by the number of cation vacancies, then the results of both Kessler et al., and of Kaderka would follow.

In all of these studies, the activation energy for the relaxation process is about the same as or slightly smaller than the motional activation energy for the major charge carrier present. This finds a natural explanation in the coupled-defect model, since reorientation of the pair involves jumps of the mobile charge-carrying defect around the impurity by which it has been trapped, and the activation energy for these jumps could be similar to that for jumps of the free carrier. It also finds a natural explanation in the surface layer model, where it is the jump of the free carrier, in a rather heavily doped layer, that determines the relaxation time.

In the present case, the high-conductivity layers were formed on CaF_2 by diffusing oxygen into the crystal from the atmosphere, consistent with the accepted picture [13] of anion vacancies as the rapidly moving intrinsic defect in CaF_2. Ure [13] observed the formation of oxidized layers on CaF_2 crystals heated to 1000 °C in a purified He atmosphere. He also observed the formation of very thin layers of very high conductivity on his specimens when heated during measurements to temperatures above 650 °C, although it is not clear whether the high conductivity was produced by oxygen. Jacobs [14] found a dielectric relaxation in some CaF_2 crystals accompanied by high measured conductivity. The magnitude of the relaxation was approximately independent of temperature. The activation energy reported by Jacobs was 0.74 eV, somewhat lower than that found in the present work.

Crystals such as CaF_2, in which anion vacancies are the mobile species and can be produced by dissolved oxygen, should be particularly sensitive to contamination by the atmosphere. The work of Bontinck [15] suggests that water vapor may enhance the rate of contamination. Dielectric relaxation in rare-earth-doped CaF_2 ascribed to defect pairs has exhibited activation energies ranging from 1.7 to 1.2 eV, in magnitude similar to or somewhat lower than the motional energy (1.7 eV) attributed by Ure [13] to anion interstitials. That this activation energy depends upon the dissolved cation argues in favor of the interpretation in terms of the reorientation of defect pairs, as does the observation that the magnitude of the relaxation increases with the concentration of impurity cation. On the other hand, Viegele and Bevan have interpreted the narrowing observed above 400 °C in the nmr spectrum of F [19] in CaF_2 containing 0.05 percent Sm as due to diffusion of F^- interstitials, presumably trapped at Sm^{3+} ions. They find an activation energy for the process of 0.26 eV, very much lower than that for either motion of free interstitials or of dielectric relaxation.

There appears to be sufficient similarity between the properties of the surface-layer model and the observations of dielectric relaxation made on various ionic crystals expected to contain defect pairs to suggest great care should be taken in interpreting the experiments. What appears to be dipole relaxation may in fact be due to surface layers. If the layers possess lower conductivity than that of the bulk, then the relaxation time will depend on the thickness, but for high conductivity layers this is not the case. In either case, dependence of the relaxation time upon heat treatment or other factors influencing conductivities may sometimes be used to test whether surface layers are responsible for the relaxation.

5.2. Low-Frequency Conduction

In figure 3, the straight lines for specimens A and D correspond to

$$T\sigma = (T\sigma)_0 \exp(-Q/kT).$$

Simply theory [17] equates $(T\sigma)$ to

$$T\sigma = \frac{e^2 a_0^2}{6k} n_0 \nu_0 \exp[(-(g_n + g_m)/kT)]$$

where e is the electronic charge, a_0 the unit jump distance (equal to the anion-anion distance in CaF_2 for anion vacancy motion), $n_0 \exp(-g_n/kT)$ the number of charge carriers, ν_0 a vibrational frequency $\sim 10^{13}$ sec^{-1}, and g_m the free energy of activation for motion of the charge carriers. Fitting this equation to the data for specimens A and D produces the result

	n_0	g_n+g_m
Specimen A (bulk)	$4.4 \times 10^{24}/cm^3$	1.5 eV
Specimen D (oxidized layer)	$1.5 \times 10^{22}/cm^3$	0.9 eV

Ure [13] has shown that the anion vacancy is mobile, with an activation energy of ~ 0.9 eV at temperatures in the range studied here. It seems reasonable to suggest that during the course of these measurements the major charge carriers in the oxidized layers were anion vacancies whose concentrations were fixed by the amount of oxygen in the lattice. Since this was saturated, the concentration is of the order of the number of unit cells/cm^3, 2×10^{22}.

In the bulk, the defect concentrations can be expected to be dominated by the GdF_3 present. On the basis of Ure's results, the mobile species in our temperature range is again expected to be the anion vacancy. In the presence of the large concentration of GdF_3 (0.1 mole percent) and assuming strong association between Gd^{3+} ions and F^- interstitials, the anion vacancy concentration should be

$$n=\frac{2N\exp\left[-(g_f-g_p/2)/kT\right]}{6\left[\text{mole fraction } Gd^{3+}\right]^{1/2}}$$

where N is the number of unit cells/cm^3, g_f the anion Frenkel formation free energy, and g_p the free energy of association of the Gd^{3+} ions with F^- interstitials. Using the nominal mole fraction GdF_3, this produces a value for n_0 of about $5\times10^{23}/cm^3$, accounting for the fact that the observed n_0 exceeds N. However, this interpretation would equate $g_f-g_p/2$ with $1.47-0.92=0.55$ eV, which cannot be reconciled with Ure's numbers, $2.8-0.7=2.1$ eV. In his study of CaF_2 containing YF_3, Ure found in the temperature range used here that σ did not increase with Y^{3+} content and suggested that some mechanism other than volume charge transport might have dominated his measurements. He observed an activation energy for conduction in this range similar to the one found here for the bulk.

It seems probable that anion vacancies are the major charge carrier in the oxidized layer, and that in the bulk the charge carriers are related to the impurity concentration somewhat as outlined above. However, a positive identification cannot be made on the basis of the present data.

6. Summary

Surface layers differing in conductivity from the bulk are easy to produce in CaF_2, and may be common in general on ionic crystals. They are known to be responsible for dielectric relaxation effects similar to those expected from reorienting defect pairs. Such layers are produced in CaF_2 by an anneal in air during the application of Pt paste electrodes, but would probably result from any high temperature treatment of the crystal in the presence of even small amounts of oxygen or water vapor.

The layers on CaF_2 produced a relaxation dispersion in the dielectric spectrum with characteristics similar to those of dispersions associated in other work with orienting defect pairs:

(i) Temperature independent magnitude of the same order as produced by a few mole percents of dipoles

(ii) Relaxation time changing with the conductivity, or with factors such as defect or impurity concentration known to affect the conductivity

(iii) Activation energy close to the activation energy of motion of the dominant charge carrier, in this case anion vacancies.

TABLE 1. *Dimensions of* CaF_2: *0.1 percent* GdF_3 *Specimens*

Specimen	Diameter	Thickness	Layer thickness	
			Electrode, l	Outer edge, l'
A	1.760 cm	0.127 cm	Not observed	Gold electrodes
B	1.698	.254	0.030 cm	0.038 cm
C	1.981	.193	.016	.017
D	1.698	.0635	Completely precipitated	

7. References

[1.a] R. G. Breckenridge, J. Chem. Phys. **16,** 959 (1948); **18,** 913 (1950).
[b] Y. Haven, J. Chem. Phys. **21,** 171 (1953).
[c] J. S. Dryden and R. J. Meakins, Disc. Far. Soc. **23,** 39 (1957).
[d] G. D. Watkins, Phys. Rev. **113,** 91 (1959).
[e] R. W. Dreyfus, Phys. Rev. **121,** 1675 (1961).
[f] G. Jacobs, L. G. Vandewiele, and A. Hamerlinck, J. Chem. Phys. **36,** 2946 (1962).
[g] R. W. Dreyfus and R. B. Laibowitz, Phys. Rev. **135,** A1413 (1964).
[h] V. V. Krasnopevtsev, Sov. Phys.-Sol. State **4,** 1327 (1963).
[i] M. Kaderka, Czech J. Phys. **B13,** 378 (1963).
[j] A. Kessler and E. Mariani, Czech J. Phys. **B14,** 757 (1964).
[2.a] J. H. Chen and M. S. McDonough, Bull. Am. Phys. Soc. **9,** 647 (1964); **11,** 195 (1966).
[b] P. D. Southgate, Bull. Am. Phys. Soc. **11,** 195 (1966).
[3] See, for instance, R. W. Sillars, J. Instn. Elect. Engrs. **80,** 378 (1937).
[4] See, for example, A. A. Fairweather and E. J. Frost, Symposium on Insulating Materials, p. 15 (Instn. of Elect. Engrs., London, 1953).
[5] P. Debye, Polar Molecules, p. 94 (Chemical Catalog Co., New York, 1929).
[6] W. L. Phillips, Jr. and J. E. Hanlon, J. Am. Ceram. Soc. **46,** 447 (1963).
[7] K. S. Cole and R. H. Cole, J. Chem. Phys. **10,** 98 (1942).
[8] K. V. Rao and A. Smakula, J. Appl. Phys. **37,** 319 (1966).
[9] See Ref. 5, p. 29.
[10] R. J. Friauf, J. Chem. Phys. **22,** 1329 (1954).
[11] T. Ninomiya and S. Sonoike, Symposium on Photographic Sensitivity, Tokyo, p. 81, ed. S. Fujisawa (Maruzen, Tokyo, **2,** 1958).
[12] N. J. Wintle and J. Rolfe, Can. J. Phys. **44,** 965 (1966).
[13] R. W. Ure, Jr., J. Chem. Phys. **26,** 1363 (1957).
[14] G. Jacobs, J. Chem. Phys. **27,** 1441 (1957).
[15] W. Bontinck, Physica **24,** 650 (1958).
[16] W. J. Viegele and A. W. Bevan, Jr., Phys. Rev. **131,** 1585 (1963).
[17] H. G. Van Bueren, Imperfections in Crystals, p. 537 (North Holland, Amsterdam, 1961).

(Paper 71A5–465)